Ann. Geophys., 31, 1109–1114, 2013
www.ann-geophys.net/31/1109/2013/
doi:10.5194/angeo-31-1109-2013

Annales Geophysicae
Open Access

Profiles of electron temperature and B_z along Earth's magnetotail

A. V. Artemyev[1,2], A. A. Petrukovich[1], R. Nakamura[3], and L. M. Zelenyi[1]

[1]Space Research Institute, RAS, Moscow, Russian Federation
[2]UMR7328, LPC2E/CNRS – University of Orleans, Orleans, France
[3]Space Research Institute, Austrian Academy of Sciences, Graz, Austria

Correspondence to: A. V. Artemyev (ante0226@gmail.com)

Received: 18 February 2013 – Revised: 26 May 2013 – Accepted: 27 May 2013 – Published: 25 June 2013

Abstract. We study the electron temperature distribution and the structure of the current sheet along the magnetotail using simultaneous observations from THEMIS spacecraft. We perform a statistical study of 40 crossings of the current sheet when the three spacecraft THB, THC, and THD were distributed along the tail in the vicinity of midnight with coordinates $X_B \in [-30\,R_E, -20\,R_E]$, $X_C \in [-20\,R_E, -15\,R_E]$, and $X_D \sim -10\,R_E$. We obtain profiles of the average electron temperature $\langle T_e \rangle$ and the average magnetic field $\langle B_z \rangle$ along the tail. Electron temperature and $\langle B_z \rangle$ increase towards the Earth with almost the same rates (i.e., ratio $\langle T_e \rangle / \langle B_z \rangle \approx$ 2 keV/7 nT is approximately constant along the tail). We also use statistics of 102 crossings of the current sheet from THB and THC to estimate dependence of T_e and B_z distributions on geomagnetic activity. The ratio $\langle T_e \rangle / \langle B_z \rangle$ depends on geomagnetic activity only slightly. Additionally we demonstrate that anisotropy of the electron temperature $\langle T_\parallel / T_\perp \rangle \approx 1.1$ is almost constant along the tail for $X \in [-30\,R_E, -10\,R_E]$.

Keywords. Magnetospheric physics (magnetotail; plasma convection; plasma sheet)

1 Introduction

The current sheet (CS) of the near-Earth magnetotail ($-10\,R_E < X < -30\,R_E$, where R_E is the Earth radius) can be approximately considered as a 2-D structure with the main gradient along the normal direction (along Z) and the weak gradient along x-direction (GSM coordinate system is used). Configuration of the magnetotail CS controls the rate of charged particle acceleration and following injection into the inner magnetosphere (see recent reviews by Baumjohann et al., 2007; Sergeev et al., 2012, and references therein). With the multi-spacecraft Cluster mission, transverse (along Z) structure of the CS was studied in detail (especially at the distances $X \sim -20\,R_E$, where Cluster collected main statistics; see Runov et al., 2006; Artemyev et al., 2011b). Although the distribution of the magnetic field along the tail plays an important role in particle (mainly electron) acceleration, it is less investigated.

Electrons are magnetized in the magnetotail, and their motion is controlled by the global gradients of the magnetic field. One of the most effective mechanisms of electron energization is adiabatic heating in the course of the earthward convection (Lyons, 1984; Zelenyi et al., 1990). This mechanism predicts monotonic growth of electron temperature with $B_z(X)$ (i.e., with X). However, recent observations and the numerical modeling suggest that a substantial role in electron energization could be played by various transient processes (see Asano et al., 2010; Fu et al., 2011; Ashour-Abdalla et al., 2011; Fu et al., 2012; Birn et al., 2012, and references therein). To compare impacts of adiabatic heating (throughout the paper, we use this term for global betatron acceleration) and transient acceleration to the electron energization, one needs to study gradient $\partial/\partial X$ of the electron temperature and magnetic field B_z along the magnetotail.

So far, estimates of the gradient $\partial/\partial X$ in the magnetotail have been obtained by using three independent approaches: (1) small-scale gradients of the near-Earth dipolarized CS can be estimated using direct measurements of Cluster mission in 2007–2009 (Nakamura et al., 2009) or THEMIS mission in the case of specific spacecraft configuration (Saito et al., 2010; Panov et al., 2012); (2) statistical investigation can give average profiles of the main CS parameters (B_z component, plasma pressure and plasma density) along the tail (see statistics collected by AMPTE/IRM, Geotail and THEMIS spacecraft in Kan and Baumjohann, 1990; Wang et al., 2012); and (3) thermal electrons could be used as

Published by Copernicus Publications on behalf of the European Geosciences Union.

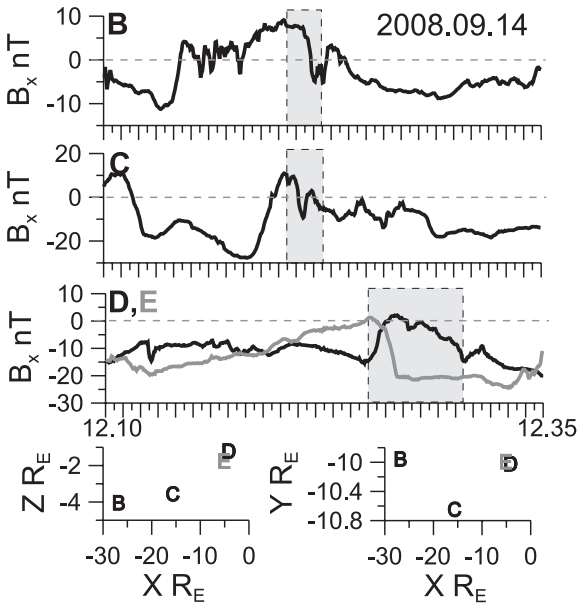

Fig. 1. Example of B_x component of the magnetic field measured by four spacecraft. Also spacecraft positions are shown.

tracers of the magnetotail structure (Artemyev et al., 2011c). The distribution of electron temperature along the magnetotail was studied only using statistical investigation (e.g., Wang et al., 2012). Each of these methods has principal disadvantages for the determination of the gradient $\partial/\partial X$ in the magnetotail: (1) direct calculation of $\partial/\partial X$ is possible only for relatively strong gradients in the dipolarized CS; (2) average profiles cannot give snapshot-like information about the magnetotail structure (the latter is important because major tail parameters vary in a wide range on timescales from minutes to hours); and (3) to use electrons as tracers, one needs realistic models of the electron heating and detailed information about the transverse structure of CS.

Therefore, existing approaches cannot be used for investigation of the relation between $T_e(X)$ and $B_z(X)$ profiles and, as a result, cannot help us study the role of electron adiabatic heating for general electron energization in the magnetotail. To obtain distribution of CS parameters along the magnetotail, the only reliable way is to organize simultaneous observations at substantially different x-coordinates. In this paper we use the statistics of simultaneous observations of thin CSs from several THEMIS spacecraft to study the relation between $T_e(X)$ and $B_z(X)$ distributions.

2 Dataset

In this study we use two datasets, which consist of THEMIS and Cluster observations, respectively. THEMIS data provide us with simultaneous observations of the magnetotail CS at different x-coordinates, while the Cluster dataset contains observations in the magnetotail for 2001–2009 from the C2 spacecraft and gives average values of T_e for several ranges of X. Due to small separation of Cluster spacecraft, we cannot use Cluster measurements for simultaneous observations of CS at different x-coordinates. The Cluster dataset includes measurements only with $|B_x| < 10$ nT and $|Y| < 5\,R_E$ (this is essentially the same dataset as the one used by Artemyev et al., 2011a).

The THEMIS statistics includes 102 events, when two spacecraft THB and THC crossed the magnetotail CS within 30 min (we consider 2008 and 2009). For 40 events from this list, THD also crossed the magnetotail CS within the same time interval. Thus, we have substatistics of 40 events with simultaneous observations at three different x-coordinates. All 102 events can be attributed to CSs with the duration of crossing varying from tens of seconds (for THB) up to tens of minutes (for THD). We cannot estimate thickness of observed CSs directly and use a criterion of rapid crossing for THB to select mainly thin CSs. For this dataset we use the magnetic field (Auster et al., 2008) and the electron measurements (McFadden et al., 2008). All data are obtained from the CDAWeb database (http://cdaweb.gsfc.nasa.gov/). For all crossings $|Y|$ coordinate is smaller than $|X|$ (i.e., all crossings occur approximately around the midnight).

A typical example of an event from THEMIS statistics is shown in Fig. 1. Grey color denotes CS crossings by the four spacecraft. THB spacecraft crossed CS; then THC and THE (as well as THD) crossed $B_x = 0$ in agreement with the distribution of z-coordinates of spacecraft. Synchronous crossings correspond to the vertical flapping motions of the CS (see the detailed study of CS flapping observed by several THEMIS spacecraft in Runov et al., 2009).

For each CS crossing from THEMIS dataset, we use the average values of $\langle T_e \rangle$, $\langle T_\parallel / T_\perp \rangle$, and $\langle B_z \rangle$ component of the magnetic field computed in the central region of CS ($|B_x| < 10$ nT), where $T_e = (T_\parallel + 2T_\perp)/3$, and $T_\parallel$ and $T_\perp$ represent diagonal components of the electron temperature tensor (smaller than $|B_x| < 10$ nT region of averaging sometimes leads to only a few points of electron data).

3 Distribution of CS parameters along the tail

We start with the statistics of 40 crossings of the magnetotail CS by three THEMIS spacecraft. For each event we have three values of $\langle T_e \rangle$ and $\langle B_z \rangle$ measured at corresponding coordinates X. Four examples of $\langle T_e \rangle$ and $\langle B_z \rangle$ distributions along the tail are shown in Fig. 2. One can see that the profiles $\langle T_e \rangle(X)$ almost coincide with the profiles $\langle B_z \rangle(X)$.

The profiles $\langle T_e \rangle$ and $\langle B_z \rangle$ along the tail for the whole THEMIS dataset are shown in Fig. 3a and c. There is a general increase of the magnetic field and the electron temperature with X (i.e., in the earthward direction). At the large distance where THB crossed the CS ($X \sim -25\,R_E$), the value of B_z is very small ($B_z \sim 1$ nT). Therefore, any deformations of the CS could result in substantial errors in estimation of B_z,

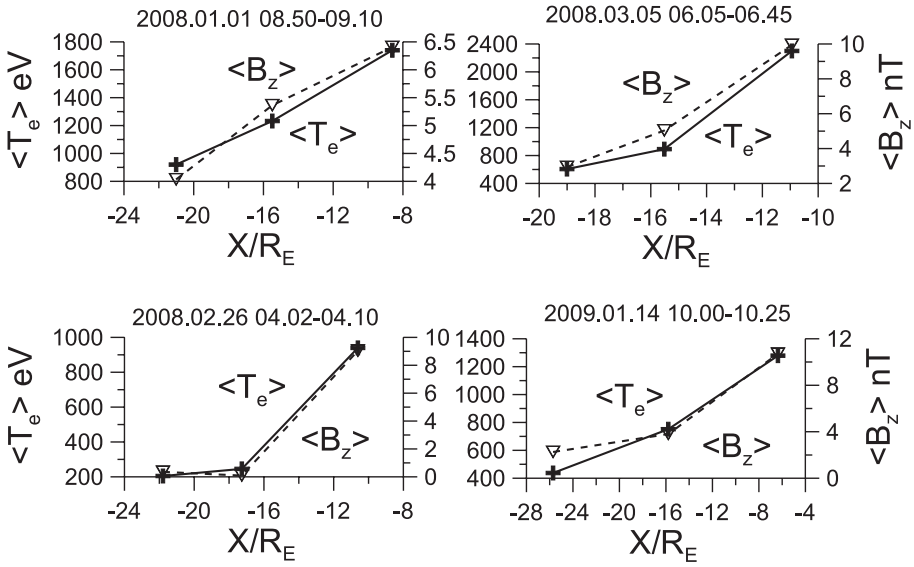

Fig. 2. Profiles of the average electron temperature $\langle T_e \rangle$ (shown by solid lines) and the magnetic field $\langle B_z \rangle$ (shown by dotted lines) along the tail.

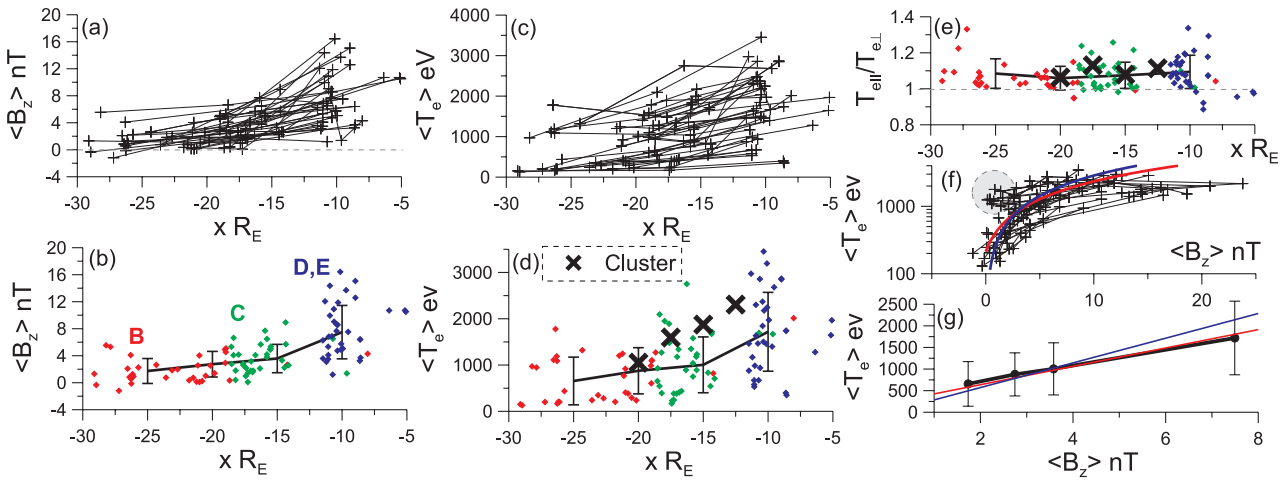

Fig. 3. $\langle T_e \rangle$, $\langle B_z \rangle$ and $\langle T_\parallel / T_\perp \rangle$ distributions in the magnetotail for 40 events, when THB, THC, and THD crossed the CS. Panels **(a)**, **(c)**, and **(f)** show all profiles of $\langle T_e \rangle$ and $\langle B_z \rangle$ from our database. In panels **(b)**, **(d)**, and **(g)**, we present average values of corresponding quantities with standard deviations. Panel **(e)** shows average values of electron temperature anisotropy. Various symbols (red, green, and blue diamonds) are used for data collected by THB, THC, and THD (THE) spacecraft. Black crosses show averaged data from Cluster C2 statistics. In panels **(f)** and **(g)**, color curves show approximations $\langle T_e \rangle / \langle B_z \rangle \approx 2\,\mathrm{keV}/7\,\mathrm{nT}$ (red curve) and $\langle T_e \rangle / (\langle B_z \rangle + 1\,\mathrm{nT}) \approx 1.7\,\mathrm{keV}/8\,\mathrm{nT}$ (blue curve). See text for details.

when the normal direction to the CS is tilted in the (X, Z) plane. This effect is clearly seen in Fig. 3f, where profiles $\langle T_e \rangle$ as function of $\langle B_z \rangle$ are shown. $\langle T_e \rangle$ mainly varies from 200 to 500 eV up to 1.5–2 keV, while $\langle B_z \rangle$ changes within the range 2–10 nT. However, there are several observations of small $\langle B_z \rangle$ with relatively large $\langle T_e \rangle$ shown by the grey circle in Fig. 3f. As a result, we cannot use the relation $\langle T_e \rangle / \langle B_z \rangle \approx$ const for the individual CS crossings.

To obtain a more reliable presentation describing profiles $\langle T_e \rangle$ and $\langle B_z \rangle$, we average our statistics for four intervals of $X \in [-10, -25]\,R_E$ (see Fig. 3b, d). Although averaging results in a loss of information regarding the peculiarities of individual cases, this operation is more accurate than collection of Cluster statistics because it takes into account only monotonic profiles of $\langle T_e \rangle$ and $\langle B_z \rangle$ along the tail. For $\langle B_z \rangle$ we obtain the following approximation based on the averaging at four intervals of X: $\langle B_z \rangle \approx 7\,\mathrm{nT} \cdot (-1 - X/5\,R_E)^{-1}$. The corresponding approximation of the electron temperature is $\langle T_e \rangle \approx 2\,\mathrm{keV} \cdot (-1 - X/5\,R_E)^{-1}$. These two approximations give the empirical proportionality $\langle T_e \rangle / \langle B_z \rangle \approx$

Table 1. Ratios of electron temperature and magnetic field. Numbers of events for three Kp range are 42, 43, and 17.

Kp	$\langle B_z^{TC}/B_z^{TB}\rangle$	$\langle T_e^{TC}/T_e^{TB}\rangle$	$\langle\Delta T_e\rangle/\langle\Delta B_z\rangle$
$\leq 1+$	1.4 ± 0.2	1.8 ± 0.05	$350/1.9\approx185$ eV/nT
2	1.75 ± 0.05	1.7 ± 0.1	$500/2.1\approx240$ eV/nT
$\geq 3-$	1.9 ± 0.1	1.8 ± 0.1	$600/2.9\approx205$ eV/nT

2 keV/7 nT (exact value is $1.9(\pm0.5)$ keV/$7.4(\pm1.2)$ nT). Due to the above-mentioned problems with small $\langle B_z\rangle$ measured by THB, the obtained temperature growth is weaker than observed growth of $\langle B_z\rangle$. Thus, the approximation $\langle T_e\rangle/\langle B_z\rangle \approx 2$ keV/7 nT slightly overestimates growth of $\langle T_e\rangle$. To correct the approximation of $\langle B_z\rangle$, we need to introduce one additional free parameter responsible for constant shift: $\langle B_z\rangle \approx -1\,\text{nT}+8\,\text{nT}\cdot(-1.3-X/4.5\,R_E)^{-0.7}$. The corresponding approximation of $\langle T_e\rangle$ profile is $\langle T_e\rangle \approx 1.7\,\text{keV}\cdot(-1.3-X/4.5\,R_E)^{-0.7}$ (exact value of $\langle T_e\rangle/(\langle B_z\rangle+1\,\text{nT})$ is $1.7(\pm0.3)$ keV/$8.1(\pm0.7)$ nT).

We plot profiles $\langle T_e\rangle$ as function of $\langle B_z\rangle$ in Fig. 3f, where red and blue curves show both our approximations. One can see that both approximations describe observations well and actually are not that different (corresponding correlation coefficients are 0.62 and 0.7). Proportionality $\langle T_e\rangle \approx (1.7\,\text{keV}/8\,\text{nT})\cdot(\langle B_z\rangle+1\,\text{nT})$ approximates data slightly better than $\langle T_e\rangle/\langle B_z\rangle \approx 2$ keV/7 nT (see Fig. 3g, where we combine the profiles from Fig. 3b, d and show $\langle T_e\rangle$ as function of $\langle B_z\rangle$). Moreover, both approximations of $\langle B_z\rangle$ coincide with AMPTE/IRM statistics presented by Kan and Baumjohann (1990) (not shown here).

We also compare measurements of electron temperature from the THEMIS mission with the Cluster dataset. Figure 3d shows Cluster C2 data of the electron temperature collected in the central region of the magnetotail CS. Cluster measurements demonstrate the growth of $\langle T_e\rangle$ with X (i.e., in the earthward direction) as well. However, the absolute values of the temperature are larger than data obtained by THEMIS. This discrepancy could be explained by different solar activity for the seasons, when Cluster and THEMIS operated in the magnetotail. Smallness of the THEMIS statistics also can be responsible for this effect.

The profile of the average electron anisotropy $T_\parallel/T_\perp$ shown in Fig. 3e demonstrates that $T_\parallel/T_\perp$ is almost constant along the tail and $T_\parallel/T_\perp \approx 1.1$ (this is a typical value of electron anisotropy; see Sergeev et al., 2001; Artemyev et al., 2011b). The same results are derived from the Cluster statistics (see large crosses in Fig. 3e). Therefore, the combination of $\langle T_e\rangle \sim \langle B_z\rangle$ and $\langle T_\parallel/T_\perp\rangle \approx$ const leads to the surprising conclusion that the parallel component of the temperature increases with the same rate as the perpendicular one ($\sim\langle B_z\rangle$). However, we should note that the variance of $T_\parallel/T_\perp$ is large. Thus, we only can conclude that temperature ratio is $T_\parallel/T_\perp \in (1, 1.2)$ without strong variation along the magnetotail.

We use full THEMIS statistics of 102 events when THB and THC crossed the magnetotail CS within short time interval. The large amount of two-point events allows us to divide these events in three groups depending on geomagnetic activity ($\text{Kp}\leq 1+$, $\text{Kp}=2$, and $\text{Kp}\geq 3-$). We do not consider the same statistics for $X > -15\,R_E$ because of the small of number of events when THB/THC and THD crossed the magnetotail CS within 30 min. For each range of Kp, we obtain average ratios $\langle B_z^{TC}/B_z^{TB}\rangle$ and $\langle T_e^{TC}/T_e^{TB}\rangle$ (Table 1). For small Kp, the increase of B_z is weaker than for $\text{Kp}\geq 2$. The ratio of temperatures is $\langle T_e^{TC}/T_e^{TB}\rangle \sim 1.8$ independent of Kp.

We calculate $\Delta T_e = T_e^{TC} - T_e^{TB}$ and $\Delta B_z = B_z^{TC} - B_z^{TB}$ (distance between THB and THC is about $\sim 6\,R_E$ for events from our statistics). In this case, the approximation $T_e = \text{const}_0 B_z + \text{const}_1$ gives $\Delta T_e/\Delta B_z = \text{const}_0$. For small $\text{Kp}\leq 1$, the temperature difference $\langle\Delta T_e\rangle$ is smaller than for $\text{Kp}\geq 2$. The ratio $\langle\Delta T_e\rangle/\langle\Delta B_z\rangle$ is similar to the value 2 keV/7 nT $\sim$ 290 eV/nT obtained for $X\in[-10,-30]\,R_E$ with three-point statistics. For $\text{Kp}\leq 1$ this ratio is one and half times smaller. However, this can be the effect of small statistics. Therefore, dependencies of ratios $\langle T_e\rangle/\langle B_z\rangle$ and $\langle T_e^{TC}/T_e^{TB}\rangle$ on geomagnetic activity seem to be weak.

4 Conclusions

In conclusion, we have shown the following: (1) electron temperature in the vicinity of the neutral plane increases with $\langle B_z\rangle$ almost linearly, and (2) anisotropy of the electron temperature is almost constant along the tail for $X\in[-25\,R_E, -10\,R_E]$. Here, we note that our results can be obtained only owing to simultaneous observations of the magnetotail current sheet from several spacecraft in different X.

These two effects provide some difficulties for the simple explanation of electron energization via the adiabatic mechanism as well as via models of the transient acceleration. Profiles of magnetic field along the magnetotail do not contain any artificially (transient) large values of $\langle B_z\rangle$. Therefore, we observe in our statistics the averaged profiles of $B_z(X)$ corresponding to the quiet magnetotail configuration. If transient processes had substantial impact on the electron energization, electron temperature would not correlate with averaged $\langle B_z\rangle$ profiles in the magnetotail. Moreover, in this case $\langle T_e\rangle$ in the near-Earth region ($X\sim -15\,R_E$) would be larger than a value obtained from a simple approximation $\langle T_e\rangle/\langle B_z\rangle \approx$ const with $\langle T_e\rangle$ measured at $X\sim -25\,R_E$. In contrast, the approximation $\langle T_e\rangle/\langle B_z\rangle \sim$ const slightly overestimates growth of $\langle T_e\rangle$, and real energization is even weaker than the increase of $\langle B_z\rangle$. Thus, we can conclude that there is no evidence (direct or indirect) of a substantial role of any transient process (like reconnection and/or dipolarization) in additional energization of the thermal electron

population. Strictly speaking, this conclusion can only be applied to quiet time conditions when the averaged $\langle B_z \rangle$ profile is monotonous along the magnetotail. However, transient mechanisms still can be important for acceleration of high-energy electrons (see Asano et al., 2010; Fu et al., 2011; Ashour-Abdalla et al., 2011; Fu et al., 2012; Birn et al., 2012, and references therein).

Although the relation $\langle T_e \rangle / \langle B_z \rangle = \text{const}$ can be considered as evidence of the adiabatic heating, we also cannot use this model to describe the observed electron energization. Adiabatic heating predicts a variation of the electron temperature anisotropy. $T_\perp$ increases linearly with $\langle B_z \rangle$ according to the betatron mechanism, while the rate of $T_\parallel$ growth provided by Fermi mechanism is smaller: $T_\parallel \sim \langle B_z \rangle^{2/5}$ (see Lyons, 1984; Zelenyi et al., 1990; Artemyev et al., 2011c, and references therein). Therefore, in the simplified model of the magnetotail, one should obtain the decrease of the anisotropy $T_\parallel / T_\perp$ with the increase of $\langle B_z \rangle$ (see Artemyev et al., 2012).

Acknowledgements. We acknowledge NASA contract NAS5-02099 and V. Angelopoulos for use of data from the THEMIS Mission. We would like to thank the following people specifically: C. W. Carlson and J. P. McFadden for use of ESA data, K. H. Glassmeier, U. Auster and W. Baumjohann for the use of FGM data provided under the lead of the Technical University of Braunschweig and with financial support through the German Ministry for Economy and Technology and the German Aerospace Center (DLR) under contract 50 OC 0302. We would like to thank V. A. Sergeev and V. S. Semenov for useful discussions. The work of L. M. Zelenyi, A. V. Artemyev and A. A. Petrukovich was supported by the RF Presidential Program for State Support of Leading Scientific Schools (project no. NSh-623.2012.2.), the Russian Foundation for Basic Research (projects nos. 10-05-91001, 10-02-93114). The work of R. Nakamura was supported by Austrian Science Fund (FWF) I429-N16. Work was also supported by the European Union Seventh Framework Programme [FP7/2007-2013] under grant agreement no. 269198 – Geoplasmas (Marie Curie International Research Staff Exchange Scheme).

Guest Editor M. Balikhin thanks two anonymous referees for their help in evaluating this paper.

The publication of this article is financed by CNRS-INSU.

References

Artemyev, A. V., Baumjohann, W., Petrukovich, A. A., Nakamura, R., Dandouras, I., and Fazakerley, A.: Proton/electron temperature ratio in the magnetotail, Ann. Geophys., 29, 2253–2257, doi:10.5194/angeo-29-2253-2011, 2011a.

Artemyev, A. V., Petrukovich, A. A., Nakamura, R., and Zelenyi, L. M.: Cluster statistics of thin current sheets in the Earth magnetotail: specifics of the dawn flank, proton temperature profiles and electrostatic effects., J. Geophys. Res., 116, A0923, doi:10.1029/2011JA016801, 2011b.

Artemyev, A. V., Zelenyi, L. M., Petrukovich, A. A., and Nakamura, R.: Hot electrons as tracers of large-scale structure of magnetotail current sheets, Geophys. Res. Lett., 38, L14102, doi:10.1029/2011GL047979, 2011c.

Artemyev, A. V., Petrukovich, A. A., Nakamura, R., and Zelenyi, L. M.: Adiabatic electron heating in the magnetotail current sheet: Cluster observations and analytical models., J. Geophys. Res., 117, A06219, doi:10.1029/2012JA017513, 2012.

Asano, Y., Shinohara, I., Retinò, A., Daly, P. W., Kronberg, E. A., Takada, T., Nakamura, R., Khotyaintsev, Y. V., Vaivads, A., Nagai, T., Baumjohann, W., Fazakerley, A. N., Owen, C. J., Miyashita, Y., Lucek, E. A., and Rème, H.: Electron acceleration signatures in the magnetotail associated with substorms, J. Geophys. Res., 115, A05215, doi:10.1029/2009JA014587, 2010.

Ashour-Abdalla, M., El-Alaoui, M., Goldstein, M. L., Zhou, M., Schriver, D., Richard, R., Walker, R., Kivelson, M. G., and Hwang, K.-J.: Observations and simulations of non-local acceleration of electrons in magnetotail magnetic reconnection events, Nature Physics, 7, 360–365, doi:10.1038/nphys1903, 2011.

Auster, H. U., Glassmeier, K. H., Magnes, W., Aydogar, O., Baumjohann, W., Constantinescu, D., Fischer, D., Fornacon, K. H., Georgescu, E., Harvey, P., Hillenmaier, O., Kroth, R., Ludlam, M., Narita, Y., Nakamura, R., Okrafka, K., Plaschke, F., Richter, I., Schwarzl, H., Stoll, B., Valavanoglou, A., and Wiedemann, M.: The THEMIS Fluxgate Magnetometer, Space Sci. Rev., 141, 235–264, doi:10.1007/s11214-008-9365-9, 2008.

Baumjohann, W., Roux, A., Le Contel, O., Nakamura, R., Birn, J., Hoshino, M., Lui, A. T. Y., Owen, C. J., Sauvaud, J.-A., Vaivads, A., Fontaine, D., and Runov, A.: Dynamics of thin current sheets: Cluster observations, Ann. Geophys., 25, 1365–1389, doi:10.5194/angeo-25-1365-2007, 2007.

Birn, J., Artemyev, A. V., Baker, D. N., Echim, M., Hoshino, M., and Zelenyi, L. M.: Particle acceleration in the magnetotail and aurora, Space Sci. Rev., 173, 49–102, doi:10.1007/s11214-012-9874-4, 2012.

Fu, H. S., Khotyaintsev, Y. V., André, M., and Vaivads, A.: Fermi and betatron acceleration of suprathermal electrons behind dipolarization fronts, Geophys. Res. Lett., 381, L16104, doi:10.1029/2011GL048528, 2011.

Fu, H. S., Khotyaintsev, Y. V., Vaivads, A., André, M., Sergeev, V. A., Huang, S. Y., Kronberg, E. A., and Daly, P. W.: Pitch angle distribution of suprathermal electrons behind dipolarization fronts: A statistical overview, J. Geophys. Res., 117, A12221, doi:10.1029/2012JA018141, 2012.

Kan, J. R. and Baumjohann, W.: Isotropized magnetic-moment equation of state for the central plasma sheet, Geophys. Res. Lett., 17, 271–274, doi:10.1029/GL017i003p00271, 1990.

Lyons, L. R.: Electron energization in the geomagnetic tail current sheet, J. Geophys. Res., 89, 5479–5487, doi:10.1029/JA089iA07p05479, 1984.

McFadden, J. P., Carlson, C. W., Larson, D., Ludlam, M., Abiad, R., Elliott, B., Turin, P., Marckwordt, M., and Angelopoulos, V.: The THEMIS ESA Plasma Instrument and In-flight Calibration, Space Sci. Rev., 141, 277–302, doi:10.1007/s11214-008-9440-2, 2008.

Nakamura, R., Retinò, A., Baumjohann, W., Volwerk, M., Erkaev, N., Klecker, B., Lucek, E. A., Dandouras, I., André, M., and Khotyaintsev, Y.: Evolution of dipolarization in the near-Earth current sheet induced by Earthward rapid flux transport, Ann. Geophys., 27, 1743–1754, doi:10.5194/angeo-27-1743-2009, 2009.

Panov, E. V., Nakamura, R., Baumjohann, W., Kubyshkina, M. G., Artemyev, A. V., Sergeev, V. A., Petrukovich, A. A., Angelopoulos, V., Glassmeier, K.-H., McFadden, J. P., and Larson, D.: Kinetic ballooning/interchange instability in a bent plasma sheet, J. Geophys. Res., 117, A06228, doi:10.1029/2011JA017496, 2012.

Runov, A., Sergeev, V. A., Nakamura, R., Baumjohann, W., Apatenkov, S., Asano, Y., Takada, T., Volwerk, M., Vörös, Z., Zhang, T. L., Sauvaud, J.-A., Rème, H., and Balogh, A.: Local structure of the magnetotail current sheet: 2001 Cluster observations, Ann. Geophys., 24, 247–262, doi:10.5194/angeo-24-247-2006, 2006.

Runov, A., Angelopoulos, V., Sergeev, V. A., Glassmeier, K.-H., Auster, U., McFadden, J., Larson, D., and Mann, I.: Global properties of magnetotail current sheet flapping: THEMIS perspectives, Ann. Geophys., 27, 319–328, doi:10.5194/angeo-27-319-2009, 2009.

Saito, M. H., Hau, L.-N., Hung, C.-C., Lai, Y.-T., and Chou, Y.-C.: Spatial profile of magnetic field in the near-Earth plasma sheet prior to dipolarization by THEMIS: Feature of minimum B, Geophys. Res. Lett., 37, L08106, doi:10.1029/2010GL042813, 2010.

Sergeev, V. A., Baumjohann, W., and Shiokawa, K.: Bidirectional electron distributions associated with near-tail flux transport, Geophys. Res. Lett., 28, 3813–3816, doi:10.1029/2001GL013334, 2001.

Sergeev, V. A., Angelopoulos, V., and Nakamura, R.: Recent advances in understanding substorm dynamics, Geophys. Res. Lett., 39, L05101, doi:10.1029/2012GL050859, 2012.

Wang, C., Gkioulidou, M., Lyons, L. R., and Angelopoulos, V.: Spatial distributions of the ion to electron temperature ratio in the magnetosheath and plasma sheet, J. Geophys. Res., 117, A08215, doi:10.1029/2012JA017658, 2012.

Zelenyi, L. M., Zogin, D. V., and Büchner, J.: Quasiadiabatic dynamics of charged particles in the tail of the magnetosphere, Cosmic Research, 28, 369–380, 1990.